A Model for the Simulation of Atmospheric Turbulence

ERIK LUNDTANG PETERSEN

Meteorology Section, Danish AEC Risø, Roskilde

(Manuscript received 4 December 1975)

ABSTRACT

A method that produces realistic simulations of atmospheric turbulence is developed and analyzed. The procedure makes use of a generalized spectral analysis, often called a proper orthogonal decomposition or the Karhunen-Loève expansion.

A set of criteria, emphasizing a realistic appearance, a correct spectral shape, and non-Gaussian statistics, is selected in order to evaluate the model turbulence.

An actual turbulence record is analyzed in detail providing both a standard for comparison and input statistics for the generalized spectral analysis, which in turn produces a set of orthonormal eigenfunctions and estimates of the distributions of the corresponding expansion coefficients.

The simulation method utilizes the eigenfunction expansion procedure to produce preliminary time histories of the three velocity components simultaneously. As a final step, a spectral shaping procedure is then applied.

The method is unique in modeling the three velocity components simultaneously, and it is found that important cross-statistical features are reasonably well-behaved. It is concluded that the model provides a practical, operational simulator of atmospheric turbulence.

1. Introduction

Demands for realistic simulation of atmospheric turbulence have increased over the years because of its obvious importance in diffusion, aeronautics, wind-loading of structures, and all boundary layer processes.

The requirements for turbulence simulation schemes inevitably give rise to a compromise between the accuracy with which empirical statistical structure is represented and the feasibility of the computational scheme. A set of criteria was suggested by Dutton and Deaven (1971). Slightly modified, they are as follows:

1) The model, through variation of internal parameters, should be able to simulate the various intensities of turbulence in the atmosphere and to provide an estimate of the likelihood of occurrence of each time history. This flexibility makes it possible to generate time sequences which approach threshold (or catastrophic) intensities for the systems whose response is being studied and to estimate the probability of failure.

2) The model should produce time histories exhibiting the sequential behavior of actual turbulence.

3) The model should produce signals possessing the most notable observed statistical characteristics of actual turbulence: the non-Gaussian behavior of the density function and the exceedance statistics, and the dependence of the energy spectrum on the $-5/3$ power of the wavenumber or frequency over a wide range.

Standard methods, which filter a white noise process so that the resulting spectra resemble those of turbulence, fail to satisfy most of these criteria. Usually a linear filter is used with Gaussian white noise as input, with the result that the simulated turbulence is also a Gaussian process, clearly contradictory to observed evidence.

The direct use of observed turbulence, which obviously satisfies the last two requirements, has only limited value because the first requirement is not satisfied.

The present model is based on the proper orthogonal decomposition theorem. The first attempt to apply this theorem in the study of turbulence was apparently made by Lumley (1965). The basic theorem, given by Loève (1955), has proved useful in the study of large-scale meteorological features (e.g., Lorenz, 1956; Kutzbach, 1967). The outline for the application of the theorem in the simulation of atmospheric turbulence was given by Dutton (1968) and Dutton and Deaven (1969).

In the model, information is extracted from measured turbulence by means of Loève-Karhunen expansions and is carried by the orthogonal functions and the statistics of the expansion coefficients.

In contrast to most models, the model generates all three velocity components simultaneously, and it is found that the simulated time histories can meet most of the requirements stated above. Moreover, cross-statistics between components seem to be modeled satisfactorily at least to second order.

Readers desiring a more detailed report on the model than that given here are referred to Petersen and Dutton (1975).

2. The model

Studies by Dutton (1968, 1969b), Dutton and Deaven (1969, 1971) and Smith (1971) have emphasized the difficulties in generating the right time sequence of the empirical turbulence even if reasonably chosen statistics seem to be modeled rather well. Nevertheless, the studies also showed that a way to success might be to emphasize the creation of gust-like events in the generated series, thus simulating the so-called "surprises" of real turbulence. The current model is based on such an approach; the philosophy behind it is given in the Appendix.

We imagine turbulence to be composed of intervals of "passive turbulence" and intervals of "active turbulence." Active turbulence intervals are defined as sequences in turbulence records in which where it is observed that a gust prevails for some specific length of time T. We hypothesize further that the active turbulence is composed of a quasi-deterministic gust structure to which is added passive turbulence. Our model is a natural result: we generate a series of passive turbulence and add to it the gust structure in such a way that the passive and the active intervals become distributed as in actual turbulence records.

It is shown in the Appendix that imposing certain principles in order to find both the gust structure, as well as an economical representation of the passive turbulence, leads to the Fredholm integral equation

$$\int_0^T R(s,t)\phi_k(t)dt=\lambda_k\phi_k(s),$$

where

$$R(s,t)=E\{f(s)f(t)\}$$

is the correlation function, and $f_n(t)$ is the data in the nth interval ($t_n\leqslant t\leqslant t_n+T$) of active turbulence isolated from the actual turbulence records and redefined over the interval $(0,T)$. The expectation operation $E\{\ \}$ is performed on the ensemble $\{f_n(t)\}$, $n=1, 2, \ldots$.

The ϕ's are orthonormal eigenfunctions of the correlation function $R(s,t)$ and, under the assumptions stated above, ϕ_1 reveals the gust structure and $\phi_2, \phi_3, \ldots$ provide us with an optimal expansion of the passive turbulence over intervals of length T.

An interval of active turbulence is then represented by

$$g_A(t)=\sum_{k=1}^{N}\alpha_k\phi_k(t)$$

and an interval of passive turbulence by

$$g_P(t)=\sum_{k=2}^{N}\alpha_k\phi_k(t).$$

The probability density functions of the expansion coefficients α_k are estimated from

$$\alpha_{k,n}=\int f_n(t)\phi_k(t)dt.$$

Hence the α_k's are sampled from their respective distributions.

It is seen that the gust structure is represented by a function that is orthogonal to all the functions used in the expansion of the passive turbulence. This then obviously requires that the two processes, the gust and the passive turbulence, be orthogonal, a requirement that can only be met approximately. Then, because of a possible non-orthogonality between gust and passive turbulence, ϕ_1 is expected to give most of the gust structure plus a little of the passive turbulence, ϕ_2 some of the gust and more of the passive turbulence, and so on. To account for this, the approach in the current model is to use all the ϕ's to construct all sequences of the turbulence, but to diminish the amplitudes of the first eigenfunctions appropriately in the intervals with passive turbulence by transforming the probability density functions for the expansion coefficients.

The model is established in two parts: an analysis scheme and a generating scheme. Roughly speaking, the first scheme describes how to obtain the eigenfunctions and the second how to use them.

a. The analysis scheme

The steps in carrying out the computation are:

A1. Select one or more observed turbulence records.

A2. Select a characteristic feature in the records believed to be of importance for the intermittency of the turbulence and select the corresponding time interval T. (The feature chosen in the current model is a large gust.)

A3. Extract as many as possible time intervals containing the feature in order to construct a representative ensemble $\{f_n(t)\}$. Estimate the probability density function for the time interval between the occurrences of the feature.

A4. Subject the ensemble to a proper orthogonal decomposition to obtain eigenfunctions and expansion coefficients and estimate the appropriate probability density functions of the coefficients.

b. The generating scheme

Because the eigenfunctions have a fixed length, it is necessary to generate the turbulence in intervals of this length. From A3 we know the distribution of the time intervals between the events, and we can then isolate values from such a distribution to determine where in the generated series the feature shall occur. From the appearance of the eigenfunctions one can

estimate how much active turbulence and how much passive turbulence is explained by the first few eigenfunctions. According to this estimate the weight of these eigenfunctions is diminished in the passive intervals. The generating scheme is then as follows:

G1. Using the probability density function from A3, generate a set of random numbers to establish the sequence of intervals of active and passive turbulence.

G2. Generate the active intervals by sampling the expansion coefficients from their probability density functions (from A4), multiply the respective expansion coefficients and eigenfunctions, and add the functions together.

G3. Generate the passive intervals as above, but make appropriate transformations of the first few probability density functions.

And if necessary:

G4. Perform a spectral shaping so that the energy spectrum is proportional to the $-5/3$ power of the frequency over an appropriate range.

3. Construction of the model

The ensemble $\{f_n(t)\}$ was selected from a turbulence record that is described in the next section. It is composed of 0.10 s block-averaged values of the u, v and w components, and the total length of the record is 50 min.

The ensemble $\{f_n(t)\}$ was then selected heuristically in the following way:

1) T was chosen to be 5 s (50 data points).

2) The record was divided into 100 segments, each of length 30 s (300 data points).

3) Inside each segment, the maximum value of w was found and a 5 s interval of data centered around this value was picked from u, v and w respectively.

4) The mth ensemble function f_m was then obtained from the mth segment ($1 \leqslant m \leqslant 100$) and the function was constructed by patching together the u, v and w components sequentially, giving a record of 150 points.

In summary, one gust interval of 5 s duration occurred at random inside each sequence of 30 s length.

The numerical approximation to the Fredholm integral equation is

$$\sum R(s,t)\phi_n(t)=\lambda_n\phi_n(s), \tag{1}$$

which is the usual eigenvector equation used in principal component analysis. As a result we have

$$\mathbf{R}(s,t)=\frac{1}{m}\sum_m \mathbf{F}_m^{\mathrm{T}}(s)\mathbf{F}_m(t),$$

where T denotes transpose and $\mathbf{F}_m$ is a $1\times M$ matrix and $\mathbf{F}_m^{\mathrm{T}}$ a $M\times 1$ matrix. Since $\mathbf{F}_m$ has the structure

$$\mathbf{F}_m(t)=[u_m(1), \ldots, u_m(50), v_m(1), \ldots, v_m(50), w_m(1), \ldots, w_m(50)],$$

this gives $\mathbf{R}(s,t)$ the structure

$$\begin{bmatrix} \mathbf{UU} & \mathbf{UV} & \mathbf{UW} \\ \mathbf{VU} & \mathbf{VV} & \mathbf{VW} \\ \mathbf{WU} & \mathbf{WV} & \mathbf{WW} \end{bmatrix}$$

where, for example, $\mathbf{UV}$ is the 50×50 uv correlation matrix.

An apparently more straightforward way to perform the analysis would be to create three ensembles, one for each of the components u, v and w, and then obtain three sets of eigenfunctions by solving (1) for $\mathbf{R}(s,t)=\mathbf{UU}$, $\mathbf{VV}$ and $\mathbf{WW}$, respectively. But then we would have disregarded all cross-statistical information, and it would be difficult to introduce it into the analysis later on.

The way the eigenfunctions are constructed in this analysis, by patching together u, v and w, enables us to use all the available second-order cross-statistical information to construct the eigenfunctions. The function $\phi_1(t)$ would then give the most likely simultaneous occurrence of u, v and w during a gust in w.

The patching of ensemble functions was used by Jaspersen (1971) to analyze vertical profiles of meteorological variables.

a. The eigenvalue spectrum and the eigenfunctions

A diagonalization was performed on the 150×150 matrix $\mathbf{R}(s,t)$ giving the eigenvalue spectrum shown in

TABLE 1. Expansion statistics for the first 20 eigenfunctions.

Eigenfunction number	Expansion coefficient		Eigenvalues		
	Mean	Standard deviation		Variance explained (percent)	(accumulated percent)
1	−1.72	6.63	47.0	27.0	27.0
2	1.39	6.28	41.4	23.8	50.7
3	3.39	2.92	20.0	11.5	62.2
4	0.96	3.15	10.8	6.2	68.4
5	0.83	2.29	5.95	3.4	71.8
6	−0.22	2.21	4.92	2.8	74.7
7	0.17	2.00	3.98	2.3	76.9
8	−0.06	1.91	3.67	2.1	79.0
9	−0.09	1.70	2.89	1.7	80.7
10	0.21	1.63	2.69	1.5	82.2
11	0		2.26	1.3	83.5
12			2.20	1.3	84.8
13			2.03	1.2	86.0
14			1.68	1.0	86.9
15			1.56	0.9	87.8
16			1.46	0.8	88.7
17			1.26	0.7	89.4
18			1.19	0.7	90.1
19			1.08	0.6	90.7
20			1.04	0.6	91.3

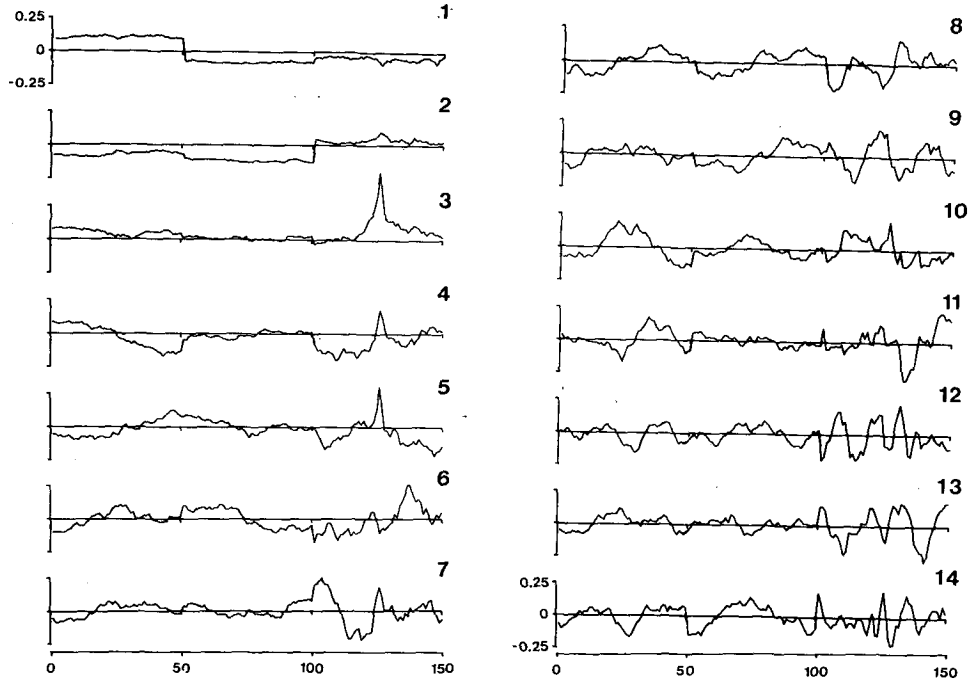

FIG. 1. First 14 eigenfunctions. Points 1–50 are the u component, points 51–100 the v component, and points 101–150 the w component.

Table 1 and the 150 eigenfunctions of which the first 14 are shown in Fig. 1.

The first two eigenfunctions seem to explain the average values of u, v and w during the "gust," and it is not surprising that this is the highest cross-correlated feature. We could have prepared the ensemble from which the eigenfunctions were calculated in such a way that the mean of u, v and w was zero in each ensemble function, or we could have removed the ensemble mean from each ensemble function. In both cases we would then have to carry some additional statistical information in the model that could be carried by the eigenfunctions and the expansion coefficient distributions themselves.

The third eigenfunction is mostly devoted to the peak in w, and to a lesser degree so are the fourth and fifth eigenfunctions. Fig. 1 reveals how the eigenfunctions, as the number increases, tend to explain features on a smaller scale.

Table 1 shows that 72% of the total variance in the ensemble is explained by the first 5 eigenfunctions, 82% by the first 10, and 91% by the first 20. The first 20 eigenfunctions were applied in the final generation scheme.

Because only 100 ensemble functions were used to create the 150×150 matrix $\mathbf{R}(s,t)$, the actual order is 99 and only 99 non-zero eigenvalues can be calculated. This creates some interdependency between the eigenfunctions. However, some degree of dependence does not seriously compromise the method.

b. The expansion coefficients

Forming a 100×150 matrix $\mathbf{F}$ of the 100 ensemble functions and a 150×20 matrix $\mathbf{E}$ of the 20 first eigenfunctions and performing the matrix multiplication

$$\mathbf{F}\times\mathbf{E}=\mathbf{B}$$

gives us the 100×20 matrix $\mathbf{B}$ consisting of the expansion coefficients α_n. A histogram is then calculated for each of the 20 columns and the corresponding probability density function estimated.

It was found subjectively that the histograms could be represented by Gaussian probability density functions, so that the only statistics necessary are the means and the variances of the 20 columns. If the ensemble had been prepared in such a way that $E\{f_n\}=0$, then

$$E\{\alpha_n\}=0,$$
$$E\{\alpha_n\alpha_k\}=\lambda_n\delta_{nk},$$

and, due to the Gaussian assumption, all the probability density functions would be known in a statistical sense, because λ_n, which equals the variance of the nth expansion coefficients, is known. In this analysis, because $E\{f_n\}\neq0$, the variance plus the squared mean of one of the expansion coefficients must equal the corresponding eigenvalue. Table 1 gives the mean and the variance for the 20 expansion coefficients. As expected, only the first few have a mean significantly different from zero.

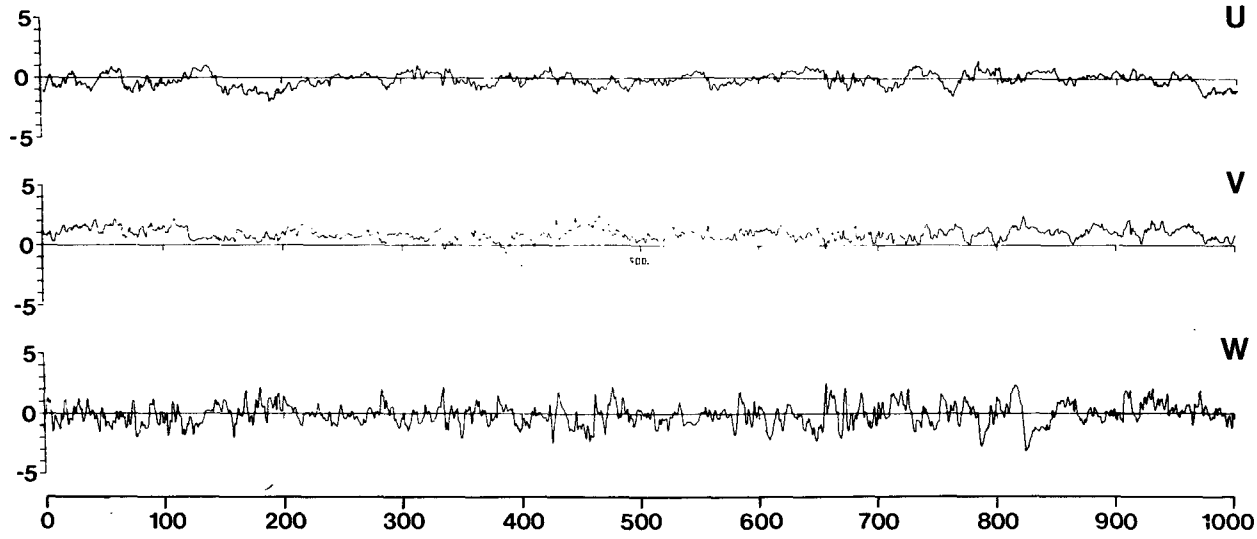

FIG. 2. Time history of Kansas turbulence data consisting of 1000 one-tenth of a second averages plotted as normalized magnitude versus time. The numbers on the horizontal axis denote tenths of seconds.

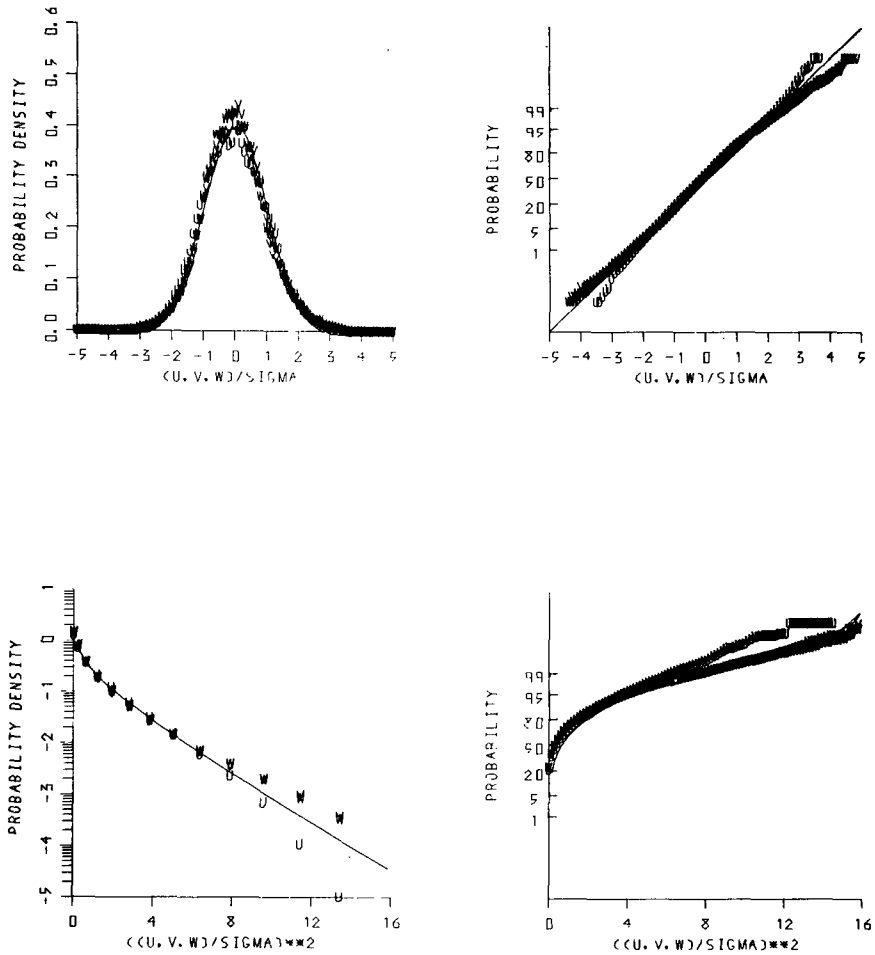

FIG. 3. Probability density and distribution functions for the first and second powers of the standardized Kansas turbulence data. The Gaussian case is illustrated by a solid line. Integers on logarithmic vertical axis denote power of 10.

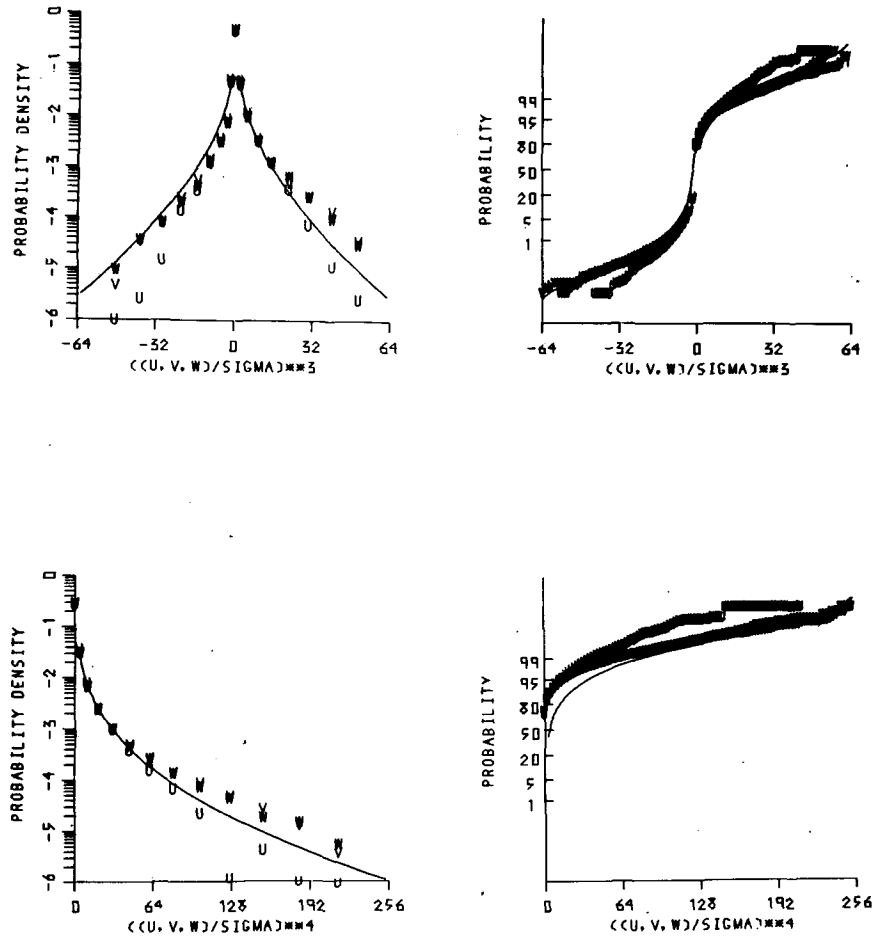

FIG. 4. As in Fig. 3 except for the third and fourth powers.

4. Description of the turbulence record

The turbulence record used here was obtained during the 1969 Kansas Experiment (Busch and Larsen, 1972). It was measured at a height of 5.66 m (from 1531 to 1631 on 30 July 1968). The stratification was slightly unstable, the Richardson number being -0.101. The mean wind speed was 6.56 m s^{-1} and the variances for the fluctuations u, v, w were 2.414, 1.904 and 0.359 m^2 s^{-2}, respectively.

The original analog data were later digitized at 1000 Hz and transferred to digital tape. For the purpose of this analysis, the signal was further block-averaged over 100 points to give a 10 Hz signal. A sequence of 50 min was selected giving 30 000 data points for each of the components u, v, w. The data were normalized to mean zero and variance 1; Fig. 2 shows 100 s of the record. The analog signal was reversed in time during the handling; thus we expect our model to generate time-reversed turbulence. A simulated record should then be time-reversed before application in practice.

In order to assess whether the generated turbulence behaves like real turbulence or not, we used the criteria given in the Introduction. One of the criteria required the model to produce signals possessing the notable observed statistical characteristics of observed turbulence. Some of these characteristics will be estimated in this section from the turbulence record, and the results will be compared with those obtained from a similar analysis by Dutton and Deaven (1971, hereafter referred to as DD).

a. Probability densities and distributions

The use of the probability functions is extended to powers of the velocity variables, here to the fourth order. Figs. 3 and 4 show the probability density and distribution functions for the standardized velocity components. In each graph, the solid line illustrates the Gaussian behavior with the curves for higher orders derived from the transformation

$$p_v(y)\left|\frac{dy}{dx}\right| = p_x(x).$$

DD reached the conclusion that the frequency functions departed from those of a Gaussian process from

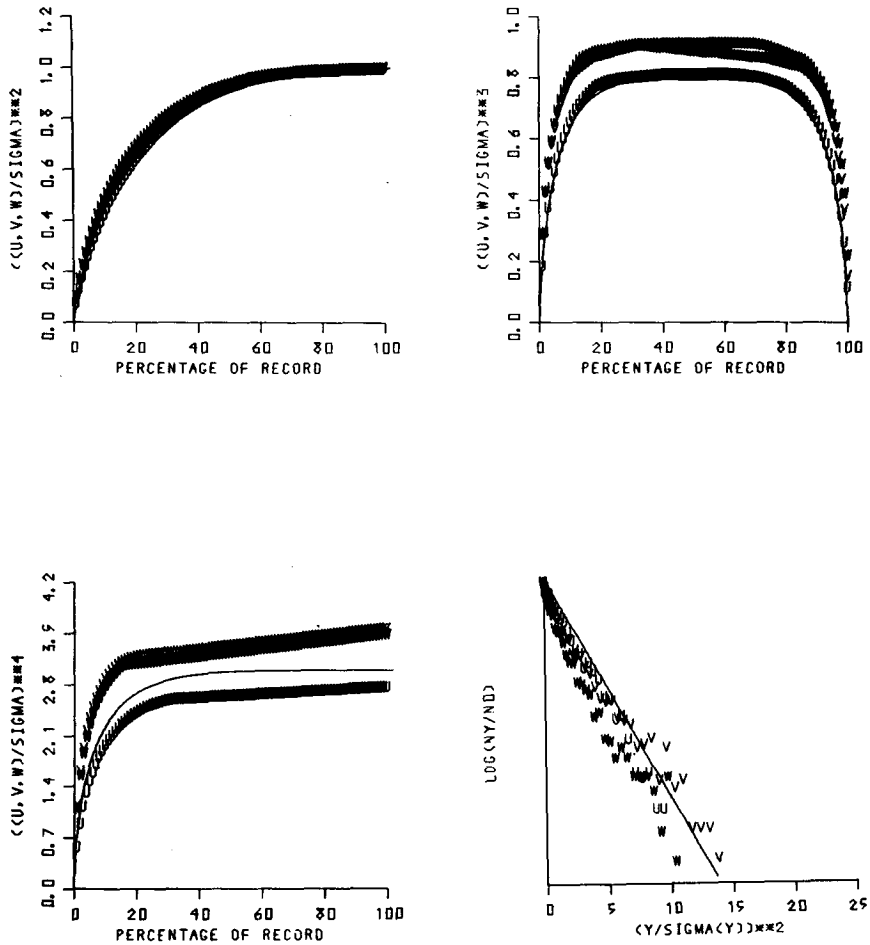

FIG. 5. Accumulation of variance, skewness and kurtosis (on the vertical axis) as a function of the percentage of the Kansas turbulence record. Note that the final symbol on the right gives the average variance, skewness and kurtosis respectively. Lower right graph: the ratio for the standardized data of the number, $N(y)$, of crossings of level y with positive slope to the number, $N(0)$, of crossings of zero with positive slope as a function of y/σ_y.

a set of figures that showed a behavior quite similar to Figs. 3 and 4.

b. Measures of intermittency

As argued by DD, the non-Gaussian behavior appears to be intimately related to the intermittency of the turbulence, and these authors provided some measures of the intermittency. Dutton (1969a) defined an intermittent process as a process where a relatively large fraction of the variance is contributed by a relatively small fraction of the total record. DD then considered how moments such as the variance, skewness and kurtosis accumulate as a function of the fraction of the total record length. These statistics are shown in Fig. 5. The numerical algorithm can be thought of as a process where first the record is rearranged so that the observations are ordered by size; the curves are then obtained by summing the appropriate power of these observations and plotting the result against the fraction of the observations used in the sum.

These figures are very similar to those given by DD with only a slight departure from the Gaussian case for the variance and a distinct deviation for the skewness and the kurtosis. The difference found between the components can also be found in some of DD's figures.

c. Exceedance statistics

Among the various exceedance statistics that can be used for studying statistical structures, DD chose $N(y)/N(0)$, which is the ratio of the number of crossings of value y with positive slope per unit time to the number of crossings of zero with positive slope. Fig. 5 shows $N(y)/N(0)$, and again we find the same behavior as found by DD.

d. Spectra and covariance functions

The analysis of turbulence relies heavily on the theory of second-order processes, the covariance functions and their Fourier transforms (the variance

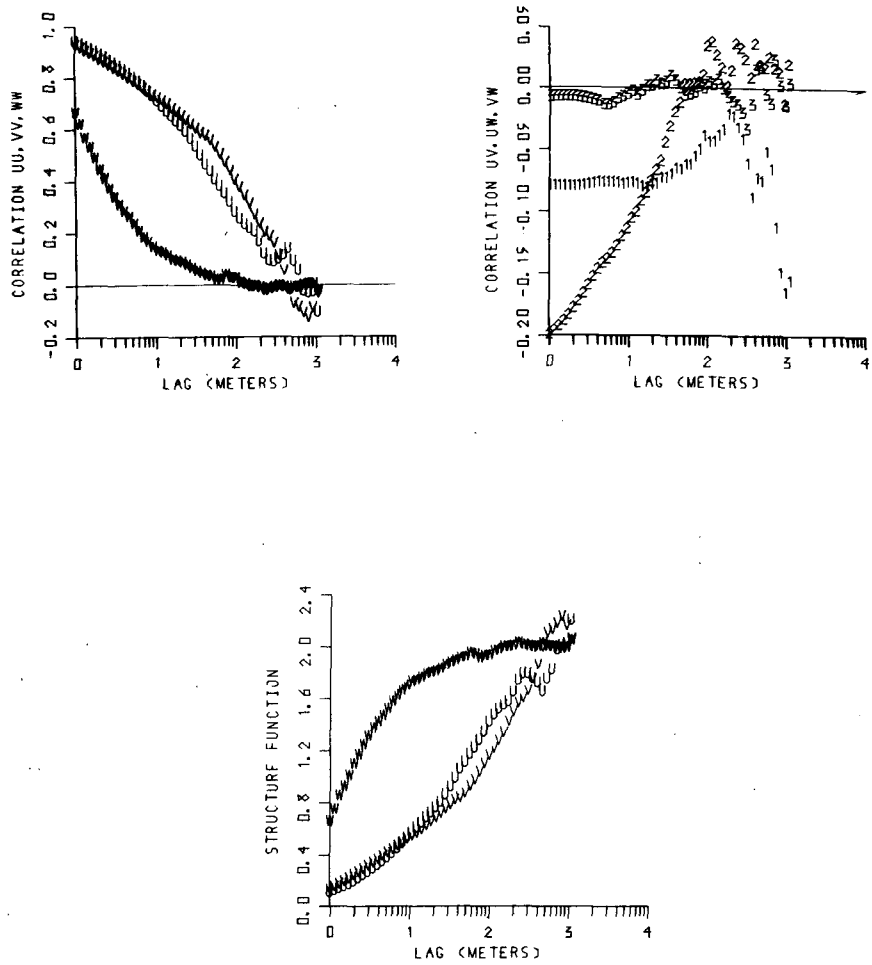

FIG. 6. Autocorrelation, crosscorrelation and structure functions for the standardized Kansas turbulence data plotted as a function of the lag on a logarithmic scale. The plotted 1 refers to the *uv* correlation functions, the 2 to *uw*, the 3 to *vw*. The integers on the horizontal axis denote power of 10.

spectra) being among the most important properties of such processes.

Although covariance functions and variance spectra contain the same information, the spectra are normally best suited for a subjective analysis because they reveal how the variance (or the covariance) is distributed over wavenumbers, and hence how the energy is distributed on scales.

The autocorrelation functions R_{uu}, R_{vv}, R_{ww} and the cross-correlation functions R_{uv}, R_{uw}, R_{vw} are shown in Fig. 6 on a logarithmic lag scale. As found by DD, the correlation of the horizontal components u and v is higher in the mid-range than that of the vertical component w. The R_{uw} function shows the expected behavior to tend to a negative value significantly different from zero at small lags indicating a downward transport of horizontal momentum (the Reynolds stress). Also shown on the figure is the structure function $D(r)$, where, for a spatially homogeneous process, the relation between $R(r)$ and $D(r)$ is easily found to be

$$D(r)=2\sigma^2[1-R(r)],$$

a relationship that can be seen to hold well for the curves on Fig. 6.

The spectra S_u, S_v, S_w and the cospectra S_{uw} are shown in Figs. 7 and 8. The most pronounced characteristic of the spectra is the $-5/3$ slope exhibited by the u and v components over one decade of frequencies. The w component is seen to flatten out at low frequencies. The cospectrum C_{uw} gives the wavenumber decomposition of the Reynolds stress responsible for the transformation of mechanical energy, and hence this is a very important statistic to model correctly. The cospectrum C_{uw} is seen to be significantly different from zero at frequencies 0.01–1, indicating that the active scales in the downward transport of momentum are of the order of 600 to 6 m. The experiment 1 spectra and co-spectra also shown in these figures are discussed in the next section.

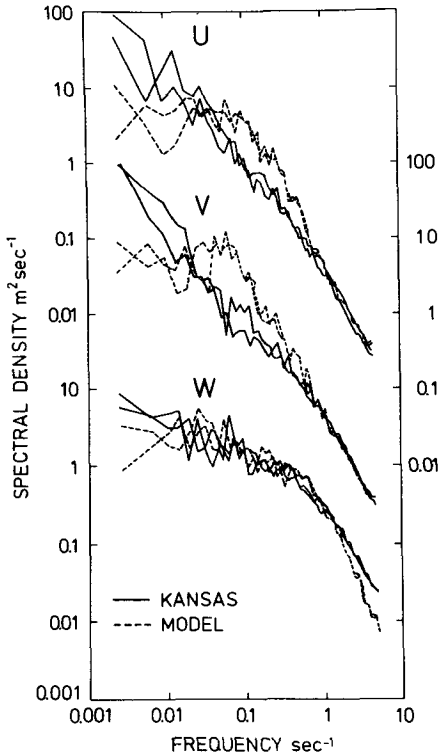

FIG. 7. Spectra of the standardized u, v and w components of two samples of Kansas turbulence, and of experiment 1. Each sample consists of 8192 points (819.2 s).

5. Testing and further development of the model

Two experiments with the model are discussed in Petersen and Dutton (1975) with the conclusion that the two sets of experimental turbulence differed no more from each other than actual turbulence records. Here the differences between the experiments will be mentioned, but only the results from experiment 1 will be discussed.

As a first step we chose to generate the series in sequences of length 30 s (300 data points). This is six times the length of one of the component parts of the eigenfunctions and our choice is obviously motivated by the way the ensemble $\{f_n(t)\}$ was constructed. Inside every 30 s interval we construct the turbulence in pieces of 5 s. One of the pieces, selected at random, represents active turbulence and the five other pieces passive turbulence.

The two experiments were performed as follows:

1. The uniformly distributed random series consisting of integers between 1 and 6 giving the position of the 5 s active turbulence piece inside the 30 s sequence is sampled for each experiment.
2. A Gaussian-distributed random series is sampled to obtain the expansion coefficients for each experiment.
3. In experiment 1, the mean and the standard deviations for the expansion coefficient distribu-

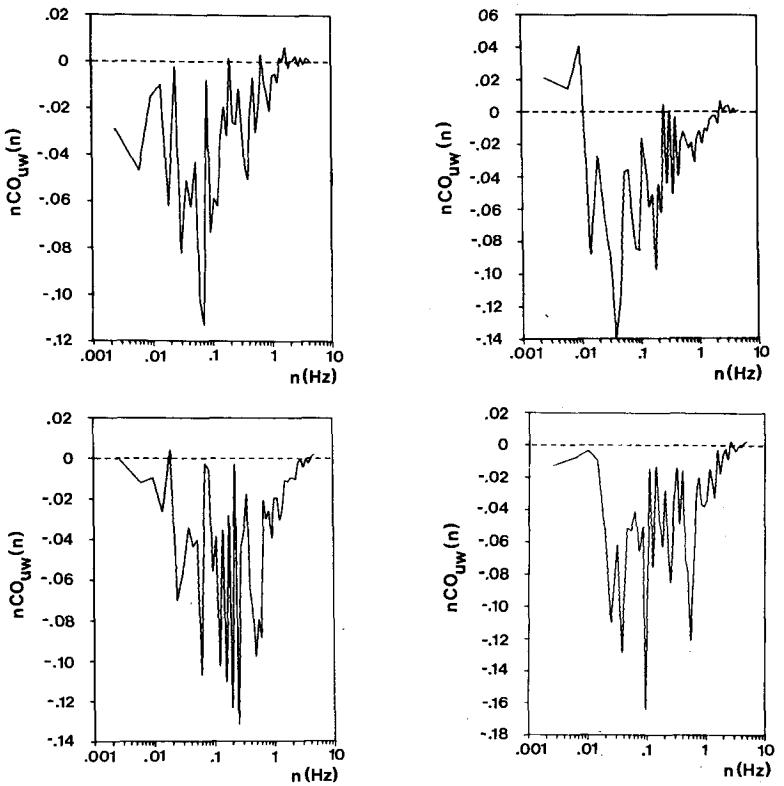

FIG. 8. Co-spectra of the standardized u and w components of two samples of Kansas turbulence (top), and experiment 1 (bottom). Each sample consists of 8192 points (819.2 s).

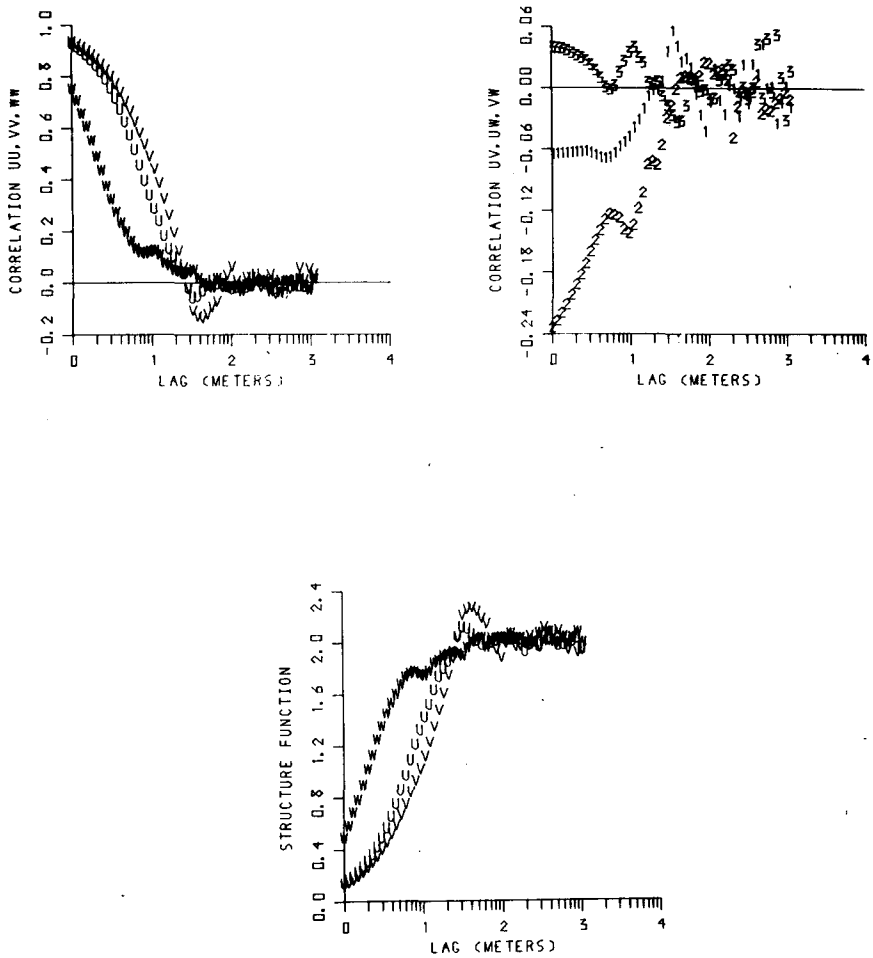

FIG. 9. Experiment 1. For further details see the legend for Fig. 6.

tions are the same as given in Table 1. In experiment 2 the standard deviations were changed to $(\sigma_1, \sigma_2, \sigma_3) = (8.0, 8.0, 4.0)$.

4. The expansion coefficients in the five passive intervals were altered by multiplying each of the three first expansion coefficients by a uniformly distributed random number between 0 and 1 for experiment 1, and 0.5 and 1 for experiment 2.

In both experiments, for every 5 s generated interval, the third expansion coefficient was multiplied by $+1$ or -1 picked at random. This procedure is justified by the shape of the eigenfunctions and the distributions of the expansion coefficients. It follows from Table 1 that, in contrast to all the other expansion coefficients, α_3 has a much larger mean than the standard deviation, implying much greater probabilities for obtaining positive rather than negative values. The shape of the third eigenfunction (Fig. 1) shows that most of its contribution is the peak in the w component that was chosen as positive when creating the ensemble $\{f_n(t)\}$. However, both negative and positive gusts should be generated and therefore the ± 1 multiplication of α_3 was introduced.

a. Static and sequential statistics of the experimental turbulence

Two times 8200 data points were generated for each component for each experiment and then subjected to the analysis applied to the turbulent record in Section 4. The full analysis is given in Petersen and Dutton (1975); the main conclusions were that the probability densities, the accumulated moments, and the exceedance curve did not differ much from those of the actual turbulence. However, discrepancies occurred when the sequential statistics were analyzed. The autocorrelations and cross correlations and the structure function are shown in Fig. 9. Comparison with Fig. 6 reveals that the experimental u and v fall off much too rapidly.

The relation between the correlation function $R(\tau)$ for a stationary time series and the corresponding correlation function $R_T(\tau)$, calculated over the length T, is given by

$$R_T(\tau) = R(\tau)\left(1 - \frac{|\tau|}{T}\right). \tag{2}$$

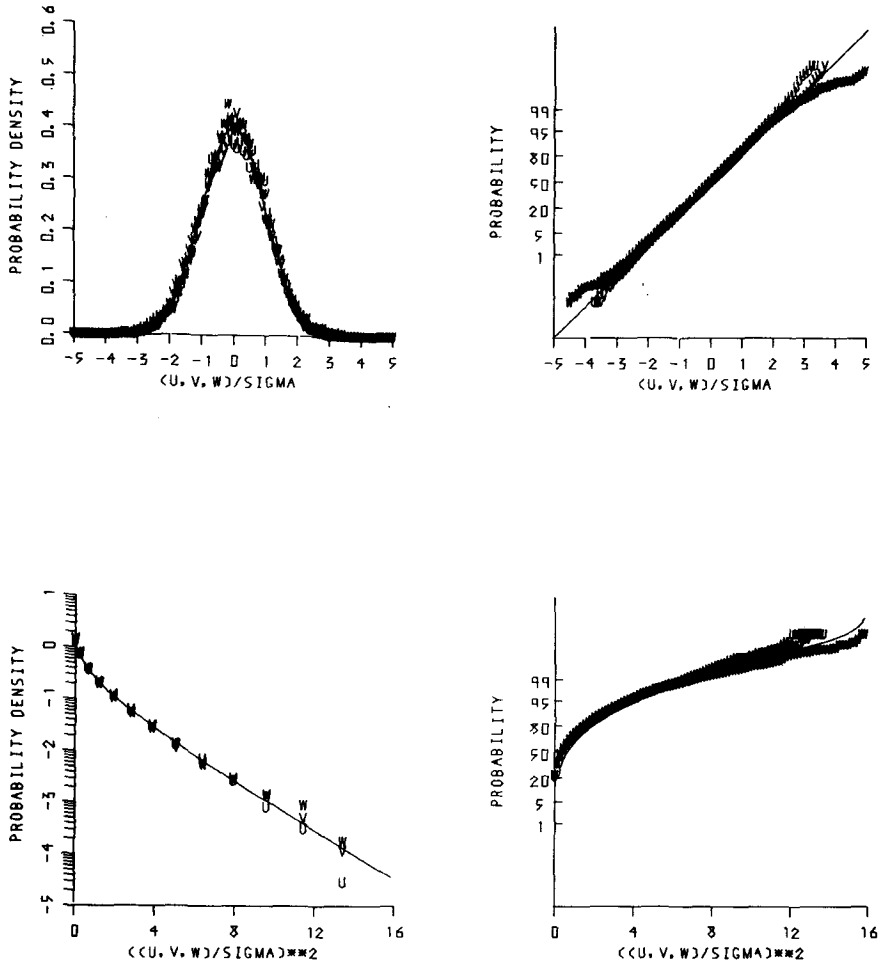

FIG. 10. Experiment 1 after spectral shaping. For further details see the legend for Fig. 3.

The generated 5 s pieces will on the average have the same correlation function as the ensemble from which the eigenfunctions were obtained. This ensemble was obtained from the turbulence record, and although it is not justifiable to call this ensemble stationary, it seems that the above transformation can explain the main differences between Figs. 6 and 9, especially when recalling that the triangle window plots as an exponential function on log-linear axes.

The generating interval was 5 s and, with a mean wind speed of 6.6 m s^{-1}, this corresponds to a length of 33 m. After a lag of 33 m the autocorrelation should thus drop to zero, which actually is the case. For the real turbulence, the zero value is reached around 600 m. With this knowledge, we would expect the generated turbulence to differ from the turbulence recorded for the u and the v components.

The cross correlations agree very well for lags of less than 30 m, and the behavior of the important uw correlation is worth emphasizing. The remarks on the autocorrelation can also be applied to the structure function.

The experimental spectra are shown in Fig. 7 together with the turbulence spectra. The u and the v spectra fall off like the turbulence spectra with a $-5/3$ slope for frequencies larger than 1 Hz. Between 1 and 0.03 Hz (scales from 6.6 to 330 m) the experimental spectra exceed the turbulence spectra, and from 0.03 Hz and less the opposite is true. We might have expected a pronounced peak in the experimental spectra at 0.2 Hz due to the generation of the turbulence in 5 s pieces, but this is not the case. The effect, if any, has been spread over more than one decade of frequencies.

The w spectra follow the same pattern, although they seem to coincide much better except for high frequencies where the experimental spectra fall off too rapidly. This probably means that the eigenfunctions from 21 and up still have some significant high-frequency features to add to w, but not to u and v.

The effect of the transformation (2), if applicable in this discussion, would be a folding of the spectra with a $(\sin\omega/\omega)^2$ function, which except for some end effects will tend to preserve power law behavior.

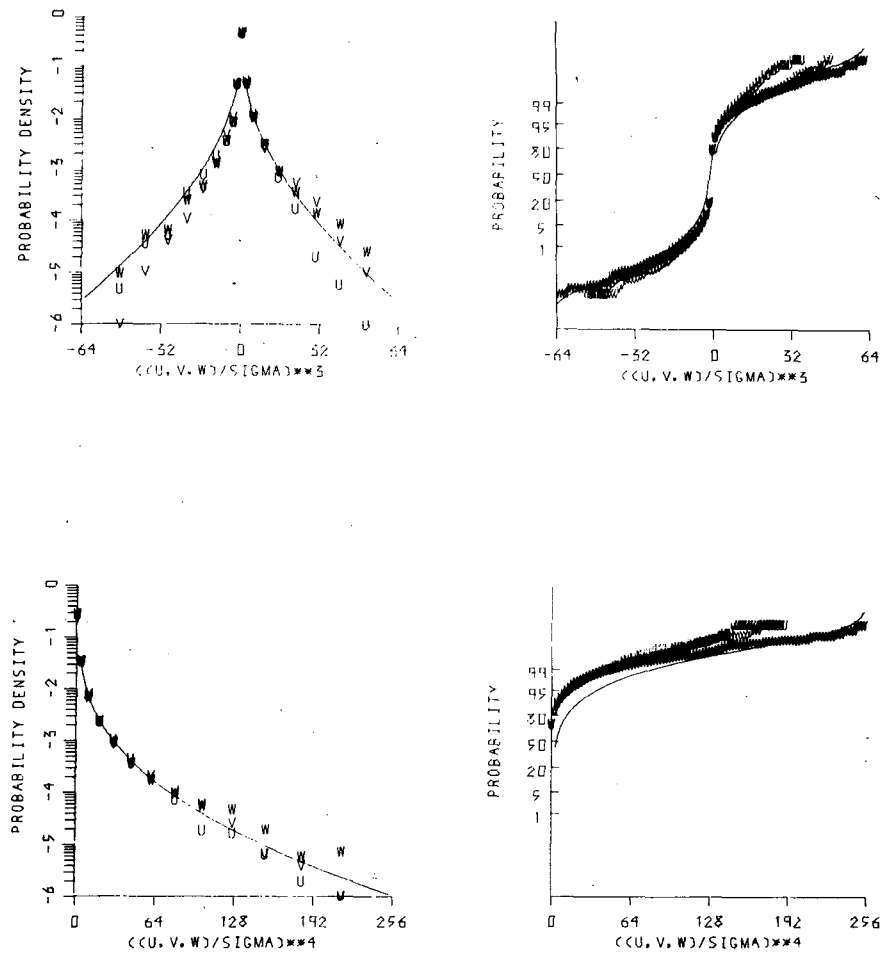

FIG. 11. Experiment 1 after spectral shaping. For further details see the legend for Fig. 4.

The agreement between the *uw* cospectra in Fig. 8 is very good.

b. Spectral shaping

In the final development of the model, some spectral shaping seems unavoidable, first because of the problems of generating energy at low wavenumbers, and second because care must be exercised in practical applications to maximize the energy at the appropriate wavenumbers.

Several methods exist, the best known one probably being to let the spectra match the behavior of the von Kármán or the Dryden spectrum (Smith, 1971; Fichtl, 1973). Another approach is to use the semi-empirical spectral formulas obtained in micrometeorological research (Busch, 1973).

The fair degree of coincidence of the measured spectra and the experimental spectra lead us to the conclusion that, in order to shape the low wavenumber ends of the experimental spectra, we could as well shape them over the whole wavenumber range using the measured spectra. This was accomplished in the following way:

Calculate the discrete Fourier transform for one component at a time and let the series of Fourier coefficients be given by

$a_0, b_0, a_1, b_1, \ldots, a_N, b_N$: the measured turbulence

$c_0, d_0, c_1, d_1, \ldots, c_N, d_N$: the generated turbulence

$e_0, f_0, e_1, f_1, \ldots, e_N, f_N$: the generated and shaped turbulence

where

$$(e_i,f_i)=\left(c_i\frac{(a_i^2+b_i^2)^{\frac{1}{2}}}{(c_i^2+d_i^2)^{\frac{1}{2}}},\quad d_i\frac{(a_i^2+b_i^2)^{\frac{1}{2}}}{(c_i^2+d_i^2)^{\frac{1}{2}}}\right),$$

which gives

$$e_i^2+f_i^2=a_i^2+b_i^2,$$

$$\frac{f_i}{e_i}=\frac{d_i}{c_i},$$

so that we have changed the spectral shape of the

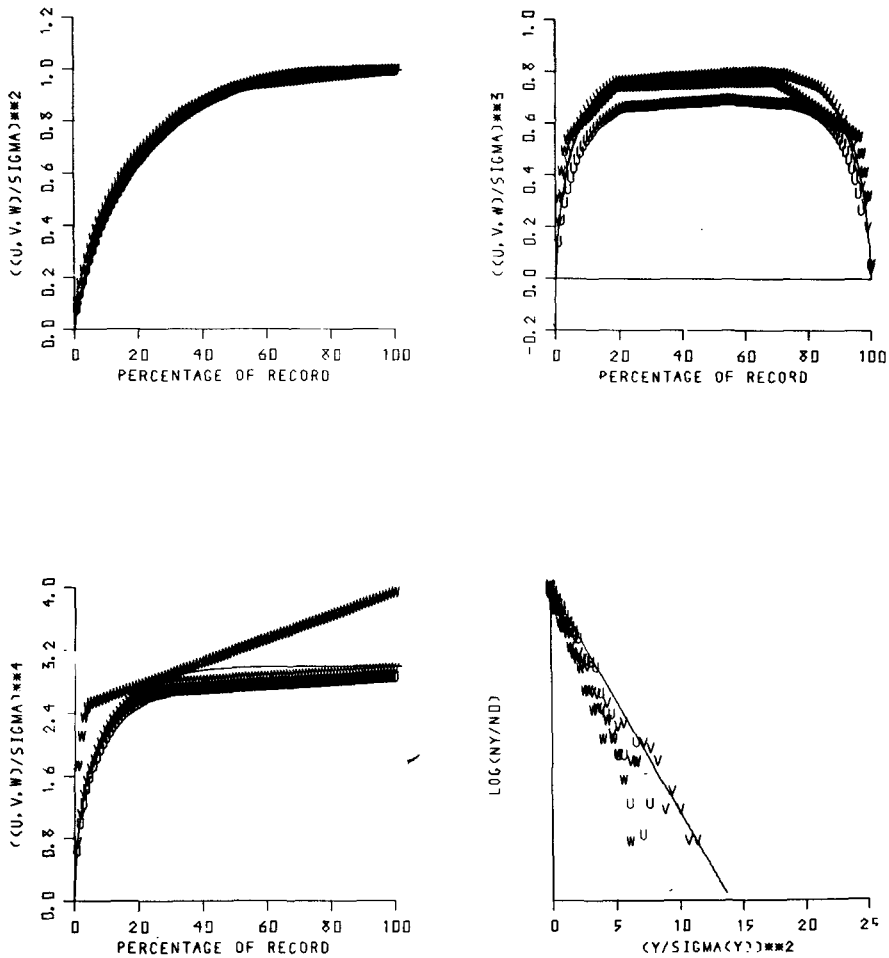

FIG. 12. Experiment 1 after spectral shaping. For further details see the legend for Fig. 5.

generated turbulence to that of the measured turbulence, but retained the phase angles from the generated series. The series (e_i, f_i) is then transformed back to obtain the series in the time domain.

The effects of the shaping are shown for Experiment 1 in Figs. 10–14. The autospectra and the autocorrelations are not shown as they must obviously be the same as for the measured record (the autocorrelation function approximately). The agreement between the various statistics for the real turbulence and the simulated turbulence is evident.

One desirable effect of the shaping is that it seemingly smooths out the effect of patching the generated 5 s pieces together, and thereby relaxes a requirement for a patching procedure.

6. Discussion

A presentation is given of an empirical turbulence model that we believe holds promise for making realistic simulations of atmospheric turbulence. This optimism stems from the fact that the model-produced turbulence has an appearance resembling that of measured turbulence and that important statistics are well modeled.

The model was created under the assumption that intermittency is a very important feature of turbulence, for which reason most effort was directed toward modeling this feature. This was accomplished by assuming that the intermittency of turbulence could be explained by considering turbulence to consist of intervals of passive turbulence and intervals of active turbulence. Measured turbulence data were then decomposed according to this assumption, and the proper orthogonal decomposition theorem was applied to the data giving statistical and sequential information about the passive and the active turbulence intervals.

The applied nature of the work, as well as limited time and computer access, forced us to predetermine many more of the important parameters in the model than necessary. The active intervals were selected so that they contained a peak in the w component in the middle of the interval. Other selection criteria could be

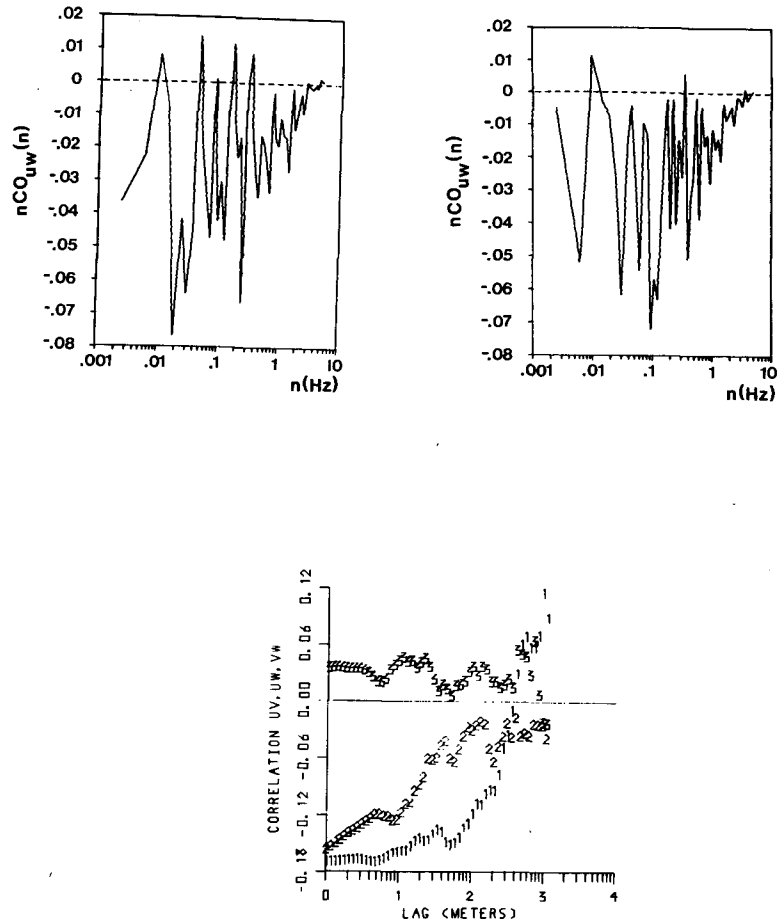

FIG. 13. Experiment 1 after spectral shaping. Top: co-spectra of two samples of the standardized u- and w-components. Each sample consists of 8192 points. Bottom: cross correlation for the standardized data plotted as functions of the lag on a logarithmic scale. The plotted 1 refers to the uv correlation, the 2 to uw, the 3 to vw. The integers on the horizontal axis denote powers of 10.

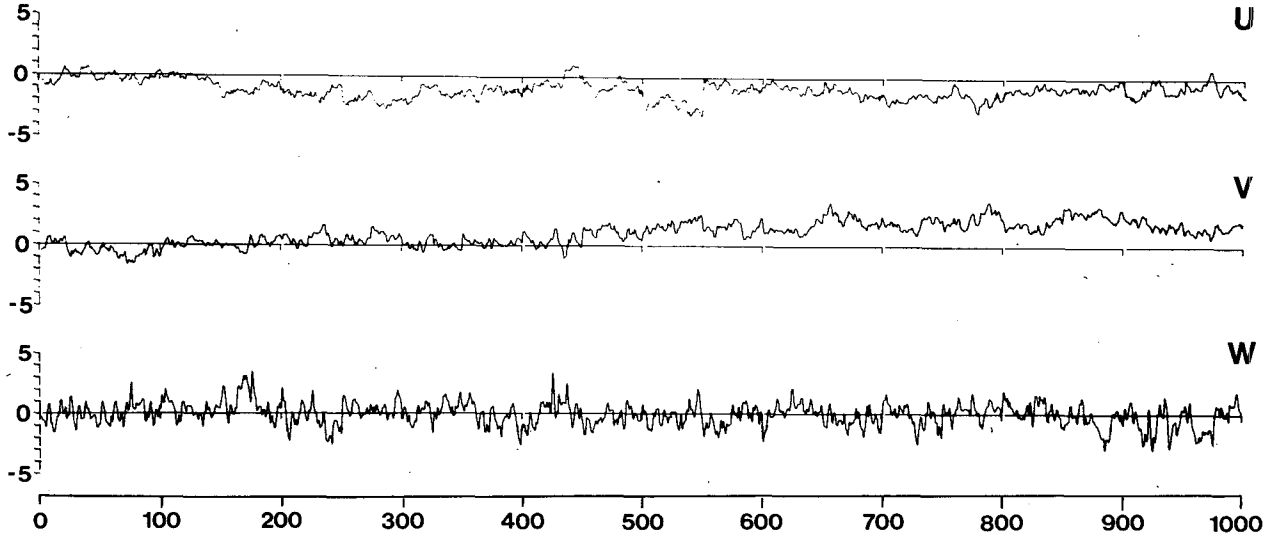

FIG. 14. Experiment 1 after spectral shaping. For further details see the legend for Fig. 2.

thought of; we tried a peak in the *uw* correlation but the results did not differ much from those of the current model. The length of the passive and active intervals should be chosen with more consideration of the integral scales of the process. The probability density function of the time interval between the active intervals should be correctly estimated from actual turbulence records. In this model both the active and the passive intervals were generated using the same set of eigenfunctions but different probability density functions for the expansion coefficients. It should be investigated whether calculation of two sets of eigenfunctions, one for each kind of interval, would lead to a better model.

The probability of occurrence of the generated turbulence is related to the particular use for which the turbulence is intended, and it is not discussed in this paper. For a short discussion see Petersen and Dutton (1975).

Acknowledgments. The research reported in this paper was supported by the U. S. National Aeronautics and Space Administration under Contract NAS8-21140 with The Pennsylvania State University. The preparation of the final manuscript was funded by the Danish Atomic Energy Commission.

All the work was done in close cooperation with Prof. John A. Dutton of The Pennsylvania State University.

APPENDIX

Theory

We are here concerned with whether quasi-deterministic behavior can be isolated if it appears in the functions in $\{f(t)\}$, where $\{f(t)\}$ is an ensemble of second order, real-valued random functions of the parameter $-\infty < t < \infty$ and where

$$\left.\begin{aligned} E\{f(t)\} &= 0 \\ E\{f^2(t)\} &= 1 \\ E\{f(s)f(t)\} &= R(s,t) \end{aligned}\right\}. \tag{A1}$$

Let $\{f_T\}$ be sub-ensembles formed from $\{f\}$ by assembling the sequential values over intervals of length T of some functions $f \in \{f\}$. For example, if

$$H(x) = \begin{cases} 1, & |x| < \dfrac{T}{2} \\ 0, & |x| \geqslant \dfrac{T}{2} \end{cases} \tag{A2}$$

then $H(x+a)f(x)$ would enter into one of the ensembles $\{f_T\}$ for every a. For ease of computation, each function in $\{f_T\}$ is redefined over the domain $(0,T)$.

If we suppose a quasi-deterministic component appears in $\{f\}$, then the question is how to select a criterion which will give a function $\phi(t)$, $0 \leqslant t \leqslant T$, that resembles the deterministic part of the functions in an optimum manner.

Several measures of resemblance are possible; the one we will choose is quadratic and has been discussed by Lumley (1965) and Dutton (1969b).

Let $\{f_T\}$ be one of the sub-ensembles of $\{f\}$. Then we define

$$\lambda = E_{\{f_T\}}\left\{\frac{\left(\int_0^T f(t)\phi(t)dt\right)^2}{\int_0^T f^2(t)dt \int_0^T \phi^2(t)dt}\right\}. \tag{A3}$$

The function ϕ we are seeking maximizes λ over the collection of all sub-ensembles $\{f_T\}$ for various values of T. Adopting other criteria in order to determine the quasi-deterministic behavior given by ϕ would in general lead to other approaches, but it is actually the criterion of (3) that brings the Karhunen-Loève expansion into the analysis, an expansion known to have some very general properties.

The question of whether there always exists a unique solution to (A3) such that it is possible to find a sub-ensemble $\{f_T\}$ determining a function $\phi(t)$, which gives an absolute maximum of λ, is considered in Petersen and Dutton (1975).

By using a first-order autoregressive series as an example, they showed that it is not always possible to find an absolute maximum of λ.

If a maximum exists, let $\{f_T\}^*$ be the associated ensemble and let $\{f_T\}\dagger$ be constructed as

$$\{f_T\}\dagger = \{f_T\} - \{f_T\}^*,$$

which is to say that $\{f_T\}\dagger$ are sub-ensembles formed from $\{f\}$ by assembling sequential values over intervals of length T which have not been used in the construction of $\{f_T\}^*$.

We will now make the assumption that almost all the information contained in $\{f\}$ can be estimated from $\phi(t)$ and $\{f_T\}\dagger$. A necessary but not a sufficient condition to fulfill this assumption is that $R(s,t)$ does not differ significantly from zero outside $|s-t| > T$. Let us further assume that we need a representation of the sequential characteristics of $\{f_T\}\dagger$ that is as economical as possible. Such a representation may be found by expanding $\{f_T\}\dagger$ with complete orthogonal systems if it is possible to find a system that gives a good approximation to the ensemble functions by an economically small number of terms.

The optimal expansion of a random function, the Karhunen-Loève expansion, is suitable for this purpose. The expansion is optimal in the sense that the series truncated at any point minimizes the integrated mean square deviation between the actual and the approximated random functions. Any other expansion using the same number of terms cannot have a smaller integrated mean square deviation. This is to say that

minimizing the error $e(N)$

$$E\{e(N)\}=E\left\{\int\left|f(t)-\sum_{n=1}^{N}\alpha_n\psi_n(t)\right|^2 dt\right\}$$

leads to an expansion (e.g., Lumley, 1965; Dutton, 1969b)

$$f(t)=\sum_{k=1}^{\infty}\alpha_k\psi_k(t), \tag{A4}$$

where the functions used in the expansion $\psi_k(t)$ are the eigenfunctions of the Fredholm integral equation

$$\int_0^T R(s,t)\psi_k(t)dt=\lambda_k\psi_k(s), \tag{A5}$$

and

$$\int \psi_k(t)\psi_l(t)dt=\delta_{kl}, \tag{A6}$$

$$E\{\alpha_n\alpha_m\}=\lambda_n\delta_{nm}, \tag{A7}$$

$$\alpha_n=\int f(t)\psi_n(t)dt, \tag{A8}$$

where the λ_n's have been arranged in a non-increasing sequence.

This follows from the Proper Orthogonal Decomposition Theorem (Loève, 1955), which states that a mean-square continuous random function $f(t)$, defined on a closed interval $0\leqslant t\leqslant T$, has the decomposition (A4) with the properties given by (A6)–(A8) if and only if λ_n are the eigenvalues and $\psi_n(t)$ the orthonormal eigenfunctions belonging to the correlation function $R(s,t)$, thus being solutions to (A5). The theory is based on Mercer's theorem, which states that a non-negative definite function $R(s,t)$, continuous over the closed interval $0\leqslant s,\ t\leqslant T$, has the expansion

$$R(s,t)=\sum_n \lambda_n\psi_n(s)\psi_n^*(t), \tag{A9}$$

where λ_n and $\psi_n(t)$ are the solutions to 5.

Solving (A5)–(A8) gives us the Karhunen-Loève expansion, sometimes referred to as a generalized spectral representation because of the lack of correlation between the coefficients of expansion.

From (A7) and (A8) we obtain

$$E\left\{\frac{1}{T}\int_0^T f^2(t)dt\right\}=\frac{1}{T}\sum_n\lambda_n,$$

which shows that the eigenvalues reveal the fraction of the total variance which is explained by the associated eigenfunction.

Our problem now is to find $\{f_T\}^*$, and thereby $\{f_T\}\dagger$, by solving the variational problem as given by (A3). Unfortunately, we are not yet able to do this in full generality, since it is not clear how to find the sub-ensemble $\{f_T\}^*$ that maximizes λ over all sub-ensembles $\{f_T\}$. However, if by some method we can establish $\{f_T\}^*$, then we can solve (A3) for the function ϕ that maximizes λ over the ensemble $\{f_T\}^*$. An approximate solution could be obtained by calculating λ and plotting it for several choices of $\{f_T\}$, but the work involved is staggering.

Let us then assume that we are able to subjectively select a sub-ensemble $\{f_T\}$ that is not far from the optimizing sub-ensemble if one exists.

Applying the techniques of the calculus of variations to (A3) to find the maximizing function, $\phi(t)$, leads to the integral equation

$$\int R(s,t)\phi_k(t)dt=\lambda_k\phi_k(s),$$

and we observe that the function most resembling each of the functions in the ensemble $\{f_T\}$ is determined by the Karhunen-Loève expansion of $\{f_T\}$; thus we have $\phi(t)=\phi_1(t)$. The expansion can be interpreted in the following way: ϕ_1 is the single function that explains the greatest variance in the ensemble, but it does not explain all the variance, so we form a new ensemble of functions $\{f_T-a_1\phi_1\}$ and find the one function most resembling the residual function. The answer will be ϕ_2 and so we consider a new ensemble $\{f_T-a_1\phi_1-a_2\phi_2\}$ and so on.

With the assumptions made we are now able to represent the sequential characteristics of $\{f\}$ by the two orthonormal systems, ψ_k and ϕ_k, together with the sampling properties of the corresponding expansion coefficients.

The two systems can be reduced to one system if further assumptions are made. For example, if the quasi-deterministic structure we are seeking occurs over the length T, if this structure is orthogonal to the rest of the process taking place over the length T, and if this structure is entirely given by the first eigenfunction ϕ_1, then the ensemble $\{f_T-a_1\phi_1\}$ will have the same properties as $\{f_T\}$. Hence ψ_1 will be the same as ϕ_2, ψ_2 as ϕ_3, and so on. Such assumptions were made in the construction of the model presented in this paper.

REFERENCES

Busch, N. E., 1973: On the mechanics of atmospheric turbulence. *Workshop on Micrometeorology*, D. A. Haugen, Ed., Amer. Meteor. Soc., 1–65.

——, and S. E. Larsen, 1972: Spectra of turbulence in the atmospheric surface layer. Risø Rep. No. 256, 187–207.

Dutton, J. A., 1968: Broadening horizons in prediction of the effects of atmospheric turbulence on aeronautical systems. AIAA Paper 68–1065.

——, 1969a: Intermittency of small-scale structure. *Radio Sci.*, 4, 1357–1359.

——, 1969b: A preliminary study of the probabilistic structure of turbulent forcing of launch vehicles. Investigation of the turbulent wind field below 150 m altitude at the Eastern Test Range, NASA Contractor Report CR-1410.

——, and D. G. Deaven, 1969: A self-similar view of atmospheric turbulence. *Radio Sci.*, 4, 1341–1349.

——, and ——, 1971: Simulation of atmospheric turbulence with empirical orthogonal functions. Statistical properties of turbulence at the Kennedy Space Center for aerospace vehicle design, NASA Contractor Report CR-1889.

——, and ——, 1971: Some observed properties of atmospheric turbulence. *Lecture Notes in Physics*, Vol. 12, *Statistical Models and Turbulence* (Proceedings of a Symposium held at the University of California, San Diego 15–21 July 1971), M. Rosenblatt and C. Van. Atta, Eds., Springer Verlag, 352–383.

Fichtl, G. H., 1973: Problems in the simulation of atmospheric boundary layer flows. *Flight in Turbulence, Proc. AGARD Flight Mechanics Panel Symposium*, Bedfordshire, United Kingdom, 1–14.

Jasperson, W., 1971: Representation of meteorological variables by empirical orthogonal functions. *Statistical Methods and Instrumentations in Geophysics*. (Proceedings of the NATO Advanced Study Institute, Norway, April 1971), A. G. Kjelas, Ed., Teknologisk Forlag, Oslo, 109–119.

Kutzbach, J. E., 1967: Empirical eigenvectors of sea level pressure, surface temperature, and precipitation complexes over North America. *J. Appl. Meteor.*, 6, 791–802.

Loève, M., 1955: *Probability Theory*. Van Nostrand, 515 pp.

Lorenz, E. N., 1956: Empirical orthogonal functions and statistical weather prediction. Sci. Rep. No. 1, Contract AF19 (604) 1566, AFCRC-TN-57-256, AD 110268.

Lumley, J. L., 1965: The structure of inhomogeneous turbulent flows. *Atmospheric Turbulence and Radio Propagation*, A. M. Yaglom and V. T. Tatarsky, Eds., Nauka, Moscow, 166–176.

Petersen, E. L., and J. A. Dutton, 1975: An application of the Karhunen-Loève expansion in simulation of atmospheric turbulence. To appear in a NASA Contractor Report.

Smith, G. W., 1971: A study in the simulation of atmospheric turbulence. M.S. thesis, Dept. of Meteorology, The Pennsylvania State University, 65 pp.